Global Biogeochemical Cycles

RESEARCH ARTICLE
10.1029/2026GB009100

Drivers and Patterns of Sediment Organic Carbon in European Regional Seas

Christian Lønborg[1], Anna Elizabeth Løvgren Graversen[2], Anna Maria Addamo[3], Jorge Assis[4], Michael Timothy Burrows[5], Eleanor Stewart[6], Helen Lillis[6], Mark John Costello[3], and Dorte Krause-Jensen[2]

[1]Department of Ecoscience, Aarhus University, Roskilde, Denmark, [2]Department of Ecoscience, Aarhus University, Aarhus, Denmark, [3]Faculty of Biosciences and Aquaculture, Nord University, Bodø, Norway, [4]Centre of Marine Sciences (CCMAR), Campus de Gambelas, Universidade do Algarve, Faro, Portugal, [5]Scottish Association for Marine Science, Oban, UK, [6]Joint Nature Conservation Committee (JNCC), Peterborough, UK

Key Points:

- Wave exposure, light availability, seabed geomorphology, and temperature drive large-scale patterns of sediment organic carbon content
- Most organic carbon occurs in low-energy coastal settings across European regional seas
- Machine learning captures regional (but not local) patterns in organic carbon content

Supporting Information:

Supporting Information may be found in the online version of this article.

Correspondence to:

C. Lønborg,
c.lonborg@ecos.au.dk;
clonborg@protonmail.com

Citation:

Lønborg, C., Graversen, A. E. L., Addamo, A. M., Assis, J., Burrows, M. T., Stewart, E., et al. (2026). Drivers and patterns of sediment organic carbon in European regional seas. *Global Biogeochemical Cycles*, *40*, e2026GB009100. https://doi.org/10.1029/2026GB009100

Received 23 JAN 2026
Accepted 29 JUL 2026

Author Contributions:

Conceptualization: Christian Lønborg, Anna Elizabeth Løvgren Graversen, Anna Maria Addamo, Jorge Assis, Dorte Krause-Jensen
Data curation: Christian Lønborg, Anna Elizabeth Løvgren Graversen, Anna Maria Addamo
Formal analysis: Christian Lønborg, Anna Elizabeth Løvgren Graversen, Anna Maria Addamo, Jorge Assis, Michael Timothy Burrows, Eleanor Stewart, Helen Lillis, Dorte Krause-Jensen
Funding acquisition: Mark John Costello, Dorte Krause-Jensen

Abstract

Mapping organic carbon (OC) stores in marine sediments is a management priority to potentially minimize the anthropogenic release of organic carbon from the seabed. Sediment OC content shows high regional variability, shaped by a complex interplay of physical, chemical, biological and anthropogenic factors. In this study, we present an assessment of the drivers and patterns of sediment OC across European regional seas, with a particular focus on the role of large-scale habitats, substratum characteristics, and environmental conditions. To investigate these relationships, we integrated data sets encompassing sediment OC, benthic habitats, sediment substrata and 11 environmental variables. Applying machine learning techniques, we identified wave exposure (estimated from wave fetch), light availability, seafloor geomorphic features, and maximum bottom water temperature as the most important environmental predictors of sediment OC content across European regional seas. While the model captured broad spatial patterns in sediment OC, it did not resolve local scale variability, making it better suited for regional assessments than for site-specific predictions. Overall, the highest OC contents were found in sediments underlying vegetated habitats such as *Posidonia oceanica* and other seagrass meadows as well as in mud, and mixed sediment substrata. OC hotspots were generally located in inshore areas with low wave fetch and temperature; these include areas of the Baltic Sea, North Sea, Adriatic Sea, Barents Sea, and the Black Sea. Our data-driven approach provides a robust foundation for identifying OC-rich sediments, which are critical for conservation planning and assessing anthropogenic impacts on marine OC.

Plain Language Summary

Marine sediments store large amounts of organic carbon. To protect these carbon stores, it is important to understand where they occur and what controls their distribution. In this study, we combined a large-scale sediment organic carbon data set with environmental data and applied machine learning to map organic carbon content across European seas. We found that carbon-rich sediments are most common in coastal areas with wave exposure, water clarity, seabed geomorphology, and temperature identified as key environmental drivers. These results provide an important tool for identifying carbon-rich areas and supporting marine conservation planning.

1. Introduction

Contemporary climate change is driven by greenhouse gas emissions from the burning of fossil fuels, which originate from organic carbon (OC) stored in soils and sediments over millions of years (Eyring et al., 2021). In the ocean, biological activity fixes carbon dioxide and transfers parts of it to the sediment (Buesseler et al., 2007). To avoid further contributing to anthropogenic greenhouse gas emissions and related climate change, it is important to reduce human activities that release and accelerate the degradation of sediment OC, such as infrastructure development, seabed dredging, fisheries bottom trawling, and mining (Epstein et al., 2022; Lønborg et al., 2024; Wu et al., 2026). Marine protected areas (MPA), where such disturbances should be prohibited, could therefore play an important role. Thus, in this study, we mapped the OC content in marine sediments to support MPA planning across all European seas.

Marine sediments play key roles in the global carbon cycle, containing around 2,322 petagrams (Pg) of OC in the top 1 m (Atwood et al., 2020). While marine sediments serve as an important OC reservoir, they are generally efficient in degrading received material, leading to low storage (from <<0.1 to 1% of the received OC) over

Investigation: Christian Lønborg, Anna Elizabeth Løvgren Graversen, Anna Maria Addamo, Jorge Assis, Michael Timothy Burrows, Mark John Costello, Dorte Krause-Jensen
Methodology: Christian Lønborg
Project administration: Mark John Costello, Dorte Krause-Jensen
Validation: Christian Lønborg, Anna Elizabeth Løvgren Graversen, Anna Maria Addamo, Jorge Assis, Michael Timothy Burrows, Eleanor Stewart, Helen Lillis, Mark John Costello, Dorte Krause-Jensen
Visualization: Christian Lønborg, Anna Elizabeth Løvgren Graversen, Anna Maria Addamo, Jorge Assis, Michael Timothy Burrows, Eleanor Stewart, Helen Lillis
Writing – original draft: Christian Lønborg
Writing – review & editing: Anna Elizabeth Løvgren Graversen, Anna Maria Addamo, Jorge Assis, Michael Timothy Burrows, Eleanor Stewart, Helen Lillis, Mark John Costello, Dorte Krause-Jensen

decades or longer (LaRowe et al., 2020; Wakeham & Canuel, 2006). In general, burial efficiency (i.e., the fraction of OC preserved) depends on both intrinsic OC characteristics (e.g., molecular structure) and external controls, including organic matter input rates, sediment accumulation rates, the hydrodynamic energy regime, and the environmental conditions to which the organic matter is exposed (Blair & Aller, 2012; Canfield, 1994). Burial efficiency typically increases from the open ocean toward inshore environments, reflecting higher organic matter supply and more rapid burial, resulting in approximately three times higher OC stocks per unit area in coastal sediments compared to the open ocean (Burdige, 2007a, 2007b).

The OC content of marine sediments is typically expressed as the percentage of the sediment dry mass (%OC). It varies widely (from <0.1% to >30%) depending on the local geomorphology, physical, chemical and biological conditions (Burdige, 2007a, 2007b). OC in marine sediments is derived from both marine and terrestrial sources, with the proportion of terrestrial material generally decreasing with distance from shore (Burdige, 2007a, 2007b). In open ocean systems, only around 25% of the OC produced in the water column reaches the sediments (Dunne et al., 2007), whereas in coastal and shelf sediments (waters <200 m depth), up to 98% can reach the sediment before being degraded (Tegler et al., 2024).

The reactivity of the sediment OC pool generally decreases with increased water depth, sediment depth and age (e.g., Smeaton & Austin, 2022; Wellsbury et al., 1997). However, OC cycling and storage are influenced by multiple intercorrelated factors, including hydrodynamic energy, organic matter chemical composition, sedimentation and supply rate, sediment fauna, flora and microbial activities, seabed lithology and granulometry, as well as the chemistry, hydrology and biology of the surrounding water column (Burdige, 2007a, 2007b). Due to this complexity, OC degradation and storage is highly variable even over smaller scales (Blair & Aller, 2012), making it challenging to disentangle the interplay between controlling factors over time and space.

The capacity of marine sediments to store OC is part of the "*blue carbon*" concept, which has been defined as "*all biologically driven carbon fluxes and storage in marine systems that are amenable to management"* (Weyer et al., 2019). Blue carbon research has focused on the management of vegetated coastal habitats to protect and potentially increase their capacity to capture carbon dioxide and retain OC while also supporting biodiversity and other key ecological functions (e.g., Howard et al., 2023). The challenges and opportunities of such "blue carbon" strategies were recently summarized (Gattuso et al., 2023; Williamson & Gattuso, 2022). Beyond the rooted coastal vegetated habitats in saltmarshes, mangroves and seagrasses, OC storage pathways and management potentials are being explored for macroalgae, tidal flats, and marine sediments in general (Howard et al., 2023). In addition to further studies on how protection may affect marine sediment OC levels, there is a need for a greater understanding of the factors controlling these and how OC levels vary across diverse seafloor habitats.

Despite decades of research, relatively few large-scale studies have attempted to link sediment OC contents and environmental drivers to determine the main regulating factors. However, several regional-scale studies have provided new insights, demonstrating that sediment OC distribution is mainly controlled by factors such as distance to the coast, sediment type, hydrodynamic energy, and sedimentation rates (e.g., Diesing et al., 2017, 2025). In this study, we utilized a recently established marine sediment OC database (Graversen et al., 2025), combined with information on environmental conditions and habitats, to identify key drivers controlling sediment OC content over large scales within European regional seas. Furthermore, it linked OC content with stocks and mapped sediment OC hot and cold spots within European regional seas. Our findings revealed how sediment OC content varies depending on environmental controls, including wave exposure, light availability, seafloor geomorphic features, and bottom-water temperature. In addition, substratum (e.g., sandy vs. muddy sediments) and habitat characteristics (e.g., seagrass meadows) further influence sediment OC content. This information may help support a more efficient conservation planning of marine environments.

2. Material and Methods

2.1. Data Compilation and Variables

For analysis and modeling, this study utilized data sourced from the sediment OC data set for European regional seas (Graversen et al., 2025), which include the Baltic Sea, the Black Sea, the North-east Atlantic Ocean, and the Mediterranean Sea. This consisted of directly determined sediment % total organic carbon (%OC) data extracted from sediment core samples, and where available, ancillary data such as temperature, habitat and water depth. This data set is compiled from direct contributions from experts and authors of previously published studies,

10.1029/2026GB009100

international and national databases, and scientific papers. Specific information required for inclusion in the final database (latitude, longitude, sediment depth intervals, and method for sediment retrieval) along with further details and a full list of ancillary data has been provided previously (Graversen et al., 2025).

Our analysis is restricted to marine sediment environments; thus, any %OC data from saltmarshes were removed due to their transitional marine-terrestrial nature, and algae meadows were also excluded due to the limited number of samples and their main occurrence in rocky habitats. Additionally, some erroneous values for dry bulk density (DBD, $n = 270$) and habitat classifications were corrected for a subset of entries ($n = 258$). Therefore, the final data set comprised 50,541 data-points with OC, which were filtered to include only the top 10 cm of the sediment. Depth-weighted averages of DBD and %OC were calculated for each core down to 10 cm. Values from individual depth intervals were weighted by their respective thicknesses, ensuring that thicker intervals contributed proportionally more to the overall average. This method accounts for unequal interval lengths. This resulted in 22,427 averaged data points. It should be noted that many sediment cores (54%) only had information regarding %OC for the top ~2 cm of sediment. Consequently, the averages (2.05% for 2 cm vs. 1.95% for 10 cm) and medians (1.30% for 2 cm vs. 1.28% for 10 cm) for these samples are, as shown in Figure S1 in Supporting Information S1, slightly higher than if information down to 10 cm had been available for all cores. However, %OC did not differ significantly between sites with interval length ≤2 cm and >2 cm (Wilcoxon rank-sum test: $W = 62{,}940{,}317$, $p = 0.240$). This %OC data set formed the basis for our analysis. Additionally, as we (a) did not identify any systematic differences in overall %OC content between vegetated and unvegetated sediments, and (b) are primarily interested in large-scale patterns, we chose to treat all data (vegetated and unvegetated) as a single combined data set in the statistical analysis.

The data set contained 1,171 paired %OC and DBD ($g*cm^{-3}$) measurements, allowing the calculation of OC standing stocks for the top 10 cm sediment layer by multiplying the weighted average %OC for those data points by their weighted average DBD. These OC stocks were then related to %OC to evaluate if the relationships for %OC also applied to OC stocks. However, as DBD was available for only a small subset of the data set, we did not use these data to estimate OC stocks across the whole study area and instead focused on %OC in our analysis. Additionally, due to the limited number of OC accumulation rate observations ($n = 89$), these data were not incorporated into our analyses of large-scale patterns.

2.2. Comparison of %OC With Seabed Habitat Classes

To investigate the relationship between seabed types and OC, we combined the European regional seas OC data set with habitat and substratum layers from the European Marine Observation and Data Network (EMODnet). Specifically, we assessed whether broad-scale seabed maps for Europe (EUSeaMap; Vasquez et al., 2023) and the EMODnet Geology seabed map (Kaskela et al., 2019) could reveal differences in the OC distribution. Two categorical variables were examined: substratum, based on the “Folk 7” sediment classification plus vegetated habitats (e.g., *Posidonia oceanica* and other seagrass meadows), and bare sediment biological zones, defined by the European Nature Information System v2007-11 classification (Davies et al., 2004). Substratum data were assigned using a hierarchical approach: habitat information from the OC database, followed by EMODnet Geology, EUSeaMap, and finally local habitat maps. In cases of missing or unlikely data (e.g., rock collected in sediment cores), alternative data sources were used. Biological zone classification followed a similar priority order, favoring local habitat maps and EUSeaMap. Data points were plotted in ArcMap 10.1 and spatial joining was used to extract this information for each individual OC data point. Once this information was merged into the %OC data set, descriptive statistics and box plots were generated to allow comparison.

2.3. Wave Exposure Model

Wave exposure of areas within 5 km of the shoreline (inshore) for Europe and the Arctic was calculated using 100-m resolution land mass data sets (Burrows et al., 2023). Offshore wave exposure was derived using a 5-km resolution land mass data set projected using UTM30N for European and Atlantic waters, and a WGS84/Arctic Polar Stereographic projection for the Arctic. Land cells were identified and excluded from further analysis. Wave exposure indices were calculated at a fine scale (50–100 m, 1–2 arcseconds) by modeling wave fetch (i.e., the distance to the nearest land in all directions) around focal grid cells using a modified version of an earlier model (Burrows, 2012; Burrows et al., 2008). The model involved searches for the nearest land around each cell over gridded search domains up to a maximum of 200 km. Initially, the minimum distance to land in each sector to the maximum wave fetch was set. For every cell in the search, the distance and angular direction from the focal coastal cell were calculated. If the cell was a land cell and the distance to that cell was less than the minimum recorded for that sector, the minimum distance for the sector was updated to the new value. Wave fetch was then expressed as the summed distance to the nearest land around each point.

2.4. Other Environmental Data

Six environmentally relevant predictor variables for the benthic realm (i.e., along the sea bottom) were extracted from the Biological and Oceanographic Rasters for Analysis of Climate and Environmental data set (Bio-ORACLE v3.0; Assis et al., 2024): maximum and minimum bottom water temperature, salinity, seawater speed, diffuse attenuation coefficient (Kd490; i.e., reduction in light intensity at 490 nm) and dissolved oxygen concentrations. These data were augmented with five additional variables: bathymetry (derived from the digital terrain model of EMODnet), slope, distance to shore, seafloor geomorphic features (Harris et al., 2014) and average annual surface runoff (Fekete et al., 2002). All environmental layers were resampled to a common resolution of 0.015° (approx. 1,670 × 1,500 m in the south; 1,670 × 290 m in the north) using bilinear interpolation, ensuring smooth transitions by averaging values from the four nearest cells. This approach standardized spatial resolution while preserving gradients in continuous data. Prior to modeling, Pearson's correlation coefficient was derived between all pairs of predictors to indicate their relationships.

2.5. Statistical Analysis

As the %OC data set was not normally distributed, as determined by the Kolmogorov–Smirnov test, the non-parametric Wilcoxon rank-sum test was used to assess whether %OC differed between the upper ∼2 cm and deeper sediment layers.

Prior to modeling, a single weighted average of %OC was assigned per 0.015° grid cell by calculating the average %OC of all the data points within each grid cell from the sediment OC data set. This resulted in 9,726 unique sites with pixel-based %OC, ranging between 0.01% and 18.30%.

The machine learning boosted regression trees (BRT) algorithm was used to model %OC against the set of predictor variables. This algorithm is renowned for its high performance, scalability, and regularization and monotonic forcing capabilities, which effectively prevent overfitting (Gouvêa et al., 2024; Lamichhane et al., 2019). The response variable was the log-transformed %OC (log (%OC + 1e−16)). Positive constraints were applied for bathymetry, the diffuse attenuation coefficient, minimum and maximum temperature, river runoff and salinity, whereas negative constraints were applied for dissolved oxygen concentrations, distance to shore, seawater speed, slope and wave fetch. To assess model robustness and quantify uncertainty, a bootstrapping procedure ($n = 7$ iterations) was employed. Within each bootstrap iteration, the data set was randomly partitioned into training (80%), validation (10%), and independent testing (10%) subsets. Hyperparameter tuning, a crucial step in machine learning, was performed using a "grid search" (Assis et al., 2022; Gouvêa et al., 2024). Models were trained with various parameter combinations (learning rate: 0.05–1.0; tree complexity: 2–6; number of trees: 50–500; minimum number of node partitioning: 1–25) on the training subset and the combination that maximized performance on the validation subset. A final model for each bootstrap iteration was then trained with the respective training data sets using these optimized hyper-parameters.

The predictive performance of each final model was assessed on its corresponding independent test set using the coefficient of determination (R^2), Pearson's correlation coefficient (r), and Root Mean Squared Error. Model interpretation involved calculating the average relative importance of each predictor variable and generating partial dependence plots for the most influential predictors, averaged across all bootstrap iterations. Finally, an ensemble prediction approach was used by applying all trained bootstrap models ($n = 7$) to the aligned environmental predictor raster stack covering the European regional seas. The pixel-wise average and standard deviation of predictions across this model ensemble were calculated and mapped to represent the final spatial estimate of %OC and its associated uncertainty. All analyses were performed in the R programming language (R Core Team, 2023). The source code is permanently available at https://github.com/jorgeassis/modellingOrganicCarbon.

Table 1
Descriptive Statistics for the Sediment Percentage Organic Carbon (%OC) Data Included in the Analysis

	Organic carbon (in %)				
	All data	≤10 cm	Bare sediment	*Posidonia oceania*	Other seagrass meadows
N	50,541	22,427	21,707	107	613
Min	<0.1	<0.1	<0.1	0.1	0.0
Max	22.1	22.1	22.1	13.3	21.0
Average	2.5	2.0	2.0	3.3	2.2
Median	1.4	1.3	1.3	1.5	0.7
IQR	2.0	2.0	2.0	5.0	2.5

Note. The number of samples (*N*), minimum (Min), maximum (Max), average, median, and Interquartile Range (IQR) are shown for all, top 10 cm, bare sediments, as well as *Posidonia oceanica* and other seagrass meadow sediments.

3. Results

3.1. Sediment Organic Carbon

Focusing on the top 10 cm across the European regional seas, the OC content ranged from <0.1 to 22.1%, with a median of 1.3% and an average of 2.0%, values consistent with the overall data set representing all sediment depths (Table 1; Figure S2 in Supporting Information S1). Most samples (97.8%) were collected from areas classified as bare sediment, whereas smaller proportions originated from seagrass meadows (2.7%, excluding *P. oceanica*) and *P. oceanica* habitats (0.5%). The DBD exhibited an exponential decline with increasing %OC across the entire data set as well as within individual habitats (Figure 1 and Figure S3 in Supporting Information S1). The fitted model tended to overestimate DBD across most of the %OC range, except at very low and very high %OC where it tended to underestimate (Figure 1 and Figure S3 in Supporting Information S1). The average calculated marine sediment OC stock in the upper 10 cm was 0.89 kg C per m^2, with an interquartile range (IQR) of 0.25–1.22 kg C per m^2, and a maximum stock of 8.75 kg C per m^2. The calculated OC stocks were positively correlated with %OC in the top 10 cm of the sediment (Figure 1 and Figure S3 in Supporting Information S1), although variability increased at higher %OC levels. Deviation from the regression line in the log-log plot of OC stocks versus %OC revealed two distinct clusters characterized by high and lower OC content, respectively (Figure 1 and Figure S3 in Supporting Information S1).

3.2. Organic Carbon Across Habitats

Using the information from EMODnet, we separated the "bare sediments" into six distinct sediment classes and five biological zones representing the gradual change in environmental conditions with depth (Tables 2 and 3; Figure 2). For the sediment classes, there was a substantial variability in %OC within each class (Table 2; Figure 2). Although the average and median were generally comparable, slightly higher average %OC were observed in "*P. oceanica*," "Seagrass meadow (other)," "mud" and mixed sediments" (Table 2). Similarly, the %OC content varied considerably across the biological zones (Table 3; Figure 2). Slightly higher average %OC were found in the "Littoral," "Infralittoral" and "shallow circalittoral" biological zones (Table 3; Figure 2).

3.3. Wave Exposure Model Results

In this study, wave exposure was calculated for coastal areas within 5 km of the shoreline, which represented 62% of the sediment %OC sampling points (13,970 out of 22,428). Overall, the geographical patterns of the average wave fetch index and wave exposure aligned with general expectations. Coastal locations had the highest average wave fetch values, whereas more wave-protected locations, such as those sheltered by islands or located further offshore, showed lower values. In particular, inlets and fjords had a notably lower wave fetch index, reflecting their sheltered position and often being close to more exposed shorelines. Additionally, offshore locations with greater water depth also tended to have lower wave fetch. The highest wave fetch values were obtained along straight open coastlines with uninterrupted exposure (Figure S4 in Supporting Information S1).

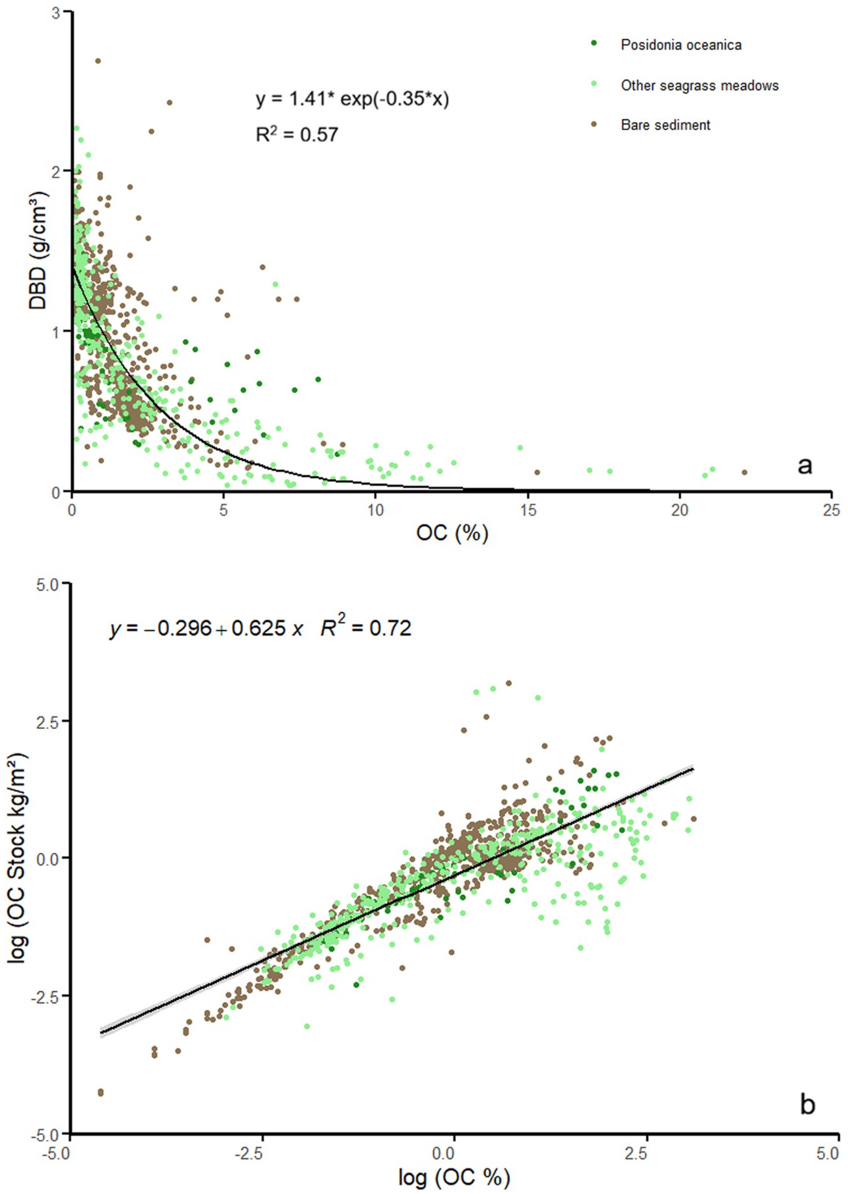

Figure 1. Relationships (a) between the percentage organic carbon content (%OC) and dry bulk density (DBD (g cm^{-3})) and (b) Log-Log relationship between %OC and calculated OC stocks (kg m^{-2}) are shown. Data from different habitats (bare sediments, *Posidonia oceania* and other seagrass meadows) are indicated by color. For habitat-specific (bare sediments, *Posidonia oceania* and other seagrass meadows) plots please see Figure S3 in Supporting Information S1.

3.4. Environmental Drivers

Our analysis of the main predictors was based on in situ observations and direct measurements of sediment %OC (Graversen et al., 2025). While the location of these data points were precise, the EMODnet substrata and habitat classifications (1:50k; Vasquez et al., 2023) and the environmental predictor variables (5-km resolution; Assis et al., 2023) were coarser in scale. This difference in spatial resolution is important to consider when interpreting the variability in %OC as it introduces uncertainty in the obtained results. Specifically, combining point-based observations with spatially gridded model outputs and climatological data sets could lead to scale-related differences, where local heterogeneity in sediment characteristics and environmental conditions is not fully captured by the larger-scale predictors. The relationship between observed and model-predicted log-transformed %OC levels showed that the model explained 53% of the deviance (Figure 3). The average relative contribution of each environmental predictor to explain the large-scale variability in %OC, derived from the BRT analysis, was used to

Table 2
Descriptive Statistics for the Sediment Percentage Organic Carbon (%OC) Data per Sediment Class (Folk 7 Classification; See Figure S7 in Supporting Information S1) and Vegetated Habitat

Sediment class	*N*	Min	Max	Average	Median	IQR
Posidonia oceanica	91	0.1	15.4	3.3	1.1	4.3
Seagrass meadow (other)	492	0.1	21.0	2.7	1.3	3.1
Mud	2441	<0.1	16.8	2.3	1.9	1.6
Sandy mud	2192	<0.1	13.9	1.5	1.1	1.3
Muddy sand	2804	<0.1	11.4	1.3	0.8	1.2
Sand	2971	<0.1	12.7	1.8	0.8	2.9
Coarse sediment	544	<0.1	6.9	0.7	0.5	0.8
Mixed sediment	539	0.1	16.8	2.3	1.7	2.3
NA	10,353	<0.1	22.1	2.3	1.5	2.2

Note. See Section 2.2 for data sources. The number of samples (*N*), minimum (Min), maximum (Max), average, median, and Interquartile Range (IQR) are shown. NA, sediment class not available.

rank the predictors (Figure 4). The most important predictor was wave fetch (32% ± 1%), followed by the diffuse (light) attenuation coefficient (14% ± 1%), seafloor geomorphic features (10% ± 1%), and maximum temperature (9% ± 1%) (Figure 4). Distance from shore, bathymetry, oxygen concentrations, and river runoff each explained between 5% and 7% of the variability (Figure 4). All other environmental predictors contributed less than 5% to the explained variation (Figure 4).

To explore the individual effects of these environmental predictors, we constructed partial dependence plots (Figure 5). These revealed that the main environmental predictor variables (wave fetch, the diffuse attenuation coefficient, seafloor geomorphic features and maximum temperature) had markedly different impacts on the %OC (Figure 5). Low wave fetch supported high %OC while increasing exposure led to a gradual decline in %OC, plateauing at high exposures (Figure 5). A higher diffuse attenuation coefficient, reflecting more turbid waters, was associated with increasing %OC, also reaching a plateau at high levels (Figure 5). %OC decreased gradually with maximum temperature up to around 25°C, followed by a stepwise decline until around 29°C (Figure 5). %OC also declined as a function of increasing distance from shore although it tended to increase with bathymetry toward deeper seafloor habitats (Figure 5). Higher %OC levels were also coupled with declining oxygen concentrations and higher river runoff (Figure 5). Differences in seafloor geomorphic features had different effects on the %OC levels, with basins, canyons and glacial troughs having a minor positive impact, whereas ridges had a negative impact (Figure 6).

Pearson's correlation matrix showed correlation coefficients (*r*) between the explanatory variables in our data set, ranging from 0 (indicates no linear relationship) to 1 (indicates a perfect positive linear relationship) and direction (±) of the relationship between the two variables. The matrix showed intercorrelation among some environmental predictor variables, such as wave fetch and bathymetry, implying that their impact could be masked because they both generally change together with distance to shore (Figure 7). This highlights the need to consider these relationships before interpreting potential cause and effect relationships.

The model-predicted map of sediment %OC across European regional seas (Figure 8a) showed higher %OC levels, especially in coastal regions, including the Baltic Sea, North Sea, Adriatic Sea, Barents Sea, and Black Sea (Figure 8a). To assess the uncertainty of the model-predicted maps, we calculated the standard deviation across the seven bootstrap model predictions, with higher values indicating less agreement among models and therefore higher associated uncertainty. Higher uncertainty, indicating lower model agreement, was observed at the edge of our study area in the mid-North Atlantic Ocean, in the Black Sea, and especially in inshore regions (Figure 8b). We also visualized spatial patterns in model error using a raster map of average prediction residuals (observed minus predicted %OC), averaged across sample location and bootstrap models (Figure S5 in Supporting Information S1). While some individual high residuals were found in the North Sea and Baltic Sea, no consistent spatial bias was evident. Boxplots of residuals by European regional seas (Figure S6 in Supporting Information S1) further confirmed that, although variability exists, there was no systematic over- or under-prediction in specific geographic areas (Figure S6 in Supporting Information S1). Thus, while the model captured general large-scale patterns, it did not fully account for the very large spatial variability in %OC.

Table 3
Descriptive Statistics for the Sediment Percentage Organic Carbon (%OC) in Bare Sediments per Biological Zone (See Davies et al. (2004) for Definitions of the Biological Zones and Section 2.2 for Data Sources)

Biological zone	*N*	Min	Max	Average	Median	IQR
Littoral	2617	<0.1	22.1	2.5	1.7	2.4
Infralittoral	2747	<0.1	16.7	2.5	1.5	3.2
Shallow circalittoral	3,256	<0.1	14.8	2.2	1.3	3.2
Deep circalittoral	8,565	<0.1	18.0	1.8	1.1	1.6
Deep sea	3,036	<0.1	16.0	1.5	1.4	1.4
NA	2206	<0.1	21.0	2.1	1.2	2.4

Note. The minimum (Min), maximum (Max), average, median, and Interquartile Range (IQR) are shown. NA, biological zone not available.

4. Discussion

The capacity of marine sediments to trap and store organic carbon (OC) varies widely across both temporal and spatial scales. This variability is driven by a complex interplay of geological, physical, chemical and biological factors both in the overlying water column and within the sediments themselves (Burdige, 2007a, 2007b). Generally, sediment OC content tends to decrease with increasing distance from shore and water depth (Burdige, 2007a, 2007b).

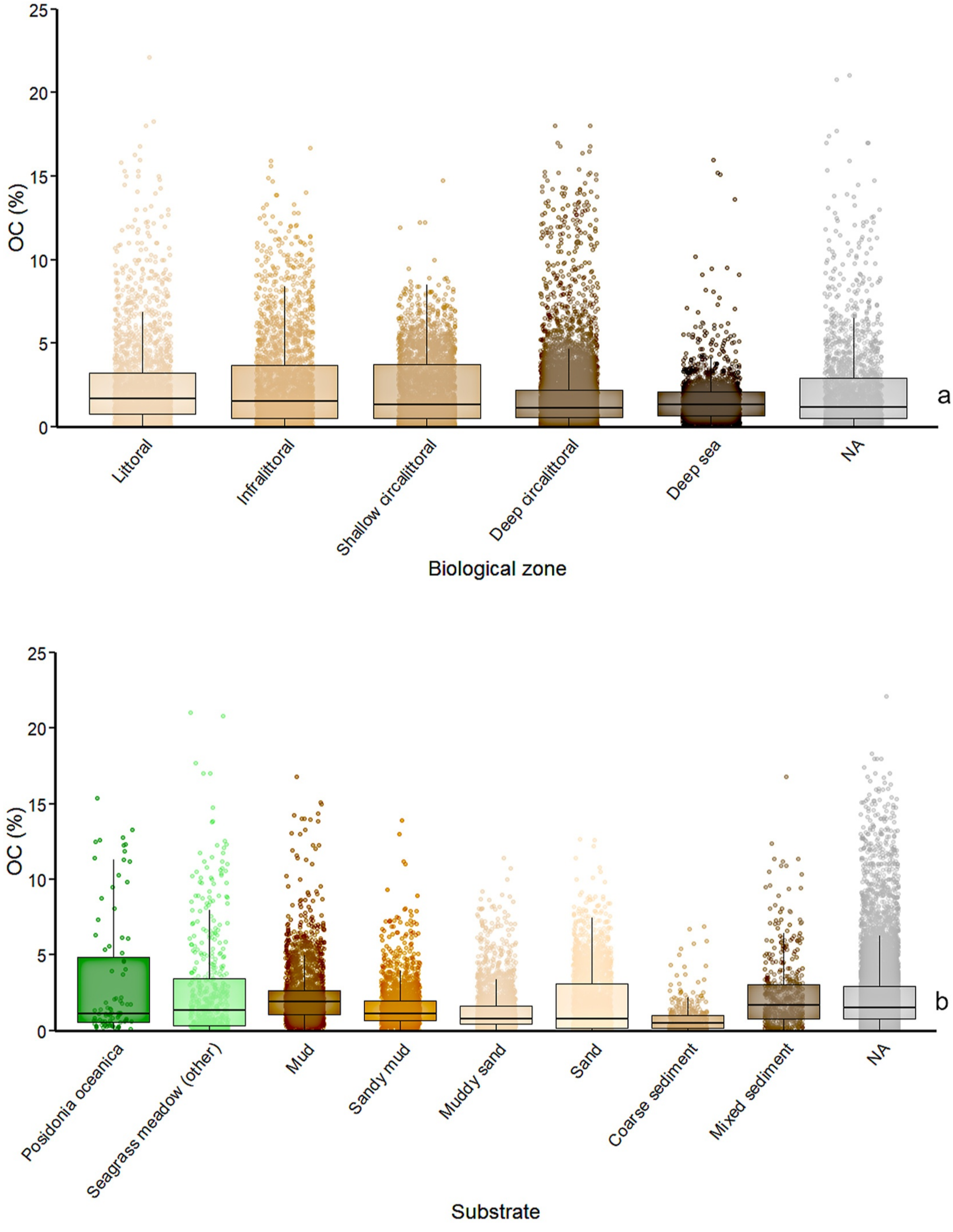

Figure 2. Boxplots of the average percentage organic carbon (%OC) for the top 10 cm sediment per (a) sediment class and vegetated habitat and (b) per biological zone. The lines in the box plot represent median values, the limits of the boxes represent 25–75 percentiles, and the whiskers represent the data range. Definitions of the sediment classes and biological zones are provided in Section 2.2 and Appendix 1 of the Supporting Information S1.

Given the high variability, identifying the key drivers of OC levels across large spatial scales remains a major challenge. In our analysis, we matched sediment OC data with environmental variables to identify potential large-scale drivers of OC distribution at the scale of European regional seas. Below, we discuss how the main predictors identified in our analysis (wave fetch, diffuse attenuation coefficient, seafloor geomorphic features, maximum

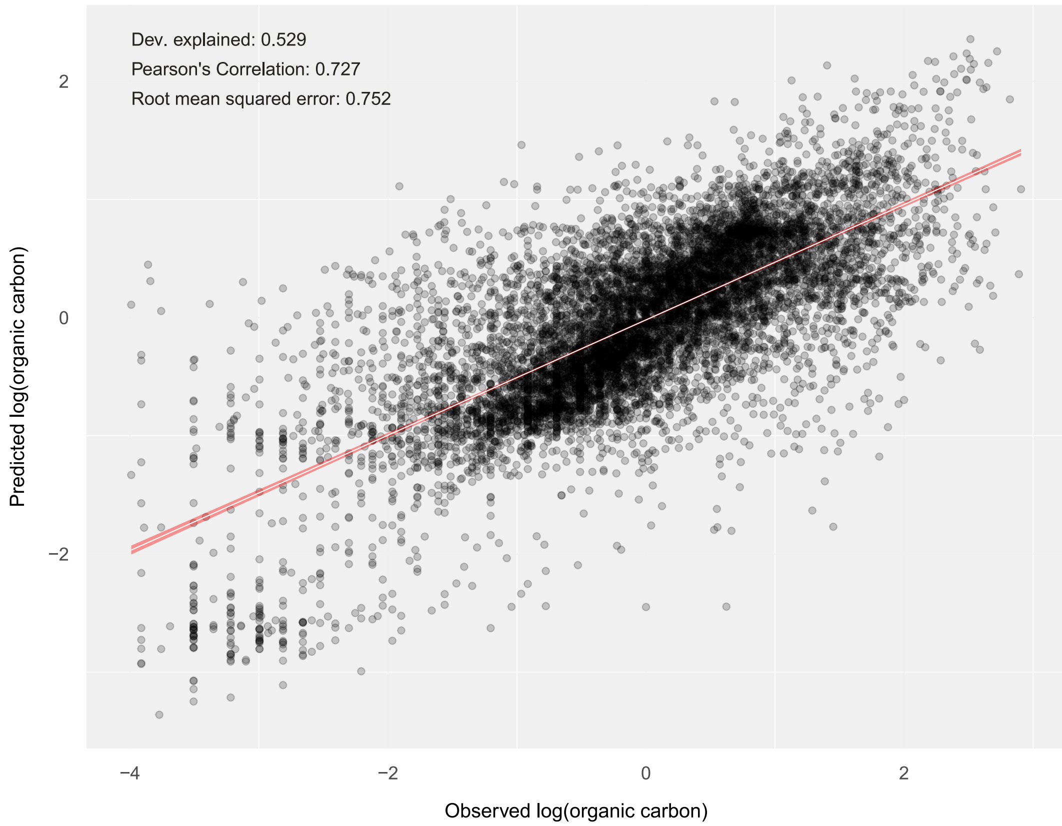

Figure 3. Relationship between the logarithm (Log-Log) of observed and model-predicted sediment percentage organic carbon (%OC; deviance explained: 0.529).

temperature) may influence sediment OC over these spatial scales, as well as the associated variability and the potentials and limitations of large-scale models and maps of sediment OC.

4.1. Drivers of Large-Scale Variability

The main predictors of sediment OC content identified in our study were broadly consistent with previous regional studies from European seas, which highlight hydrodynamic energy, sediment type, and depositional conditions as key controls (e.g., Diesing et al., 2017, 2025). The importance of wave exposure (estimated from fetch) found in this study aligns with these previous findings, reflecting the role of low bottom shear stress and low-energy environments in promoting OC accumulation. However, the relative importance of these predictors differ between studies, likely due to variations in environmental settings, spatial resolution, and predictor selection. Overall, our results showed that large-scale patterns were mainly governed by interactions between hydrodynamic conditions, local productivity, sediment properties, and seafloor geomorphology.

Among the environmental predictors analyzed, wave exposure emerged as the single most important factor explaining variation in sediment OC levels. This intuitively makes sense, as increased wave activity and current velocity, can hinder deposition, enhance erosion, and promote the degradation of sedimentary OC (de Haas et al., 2002; Lønborg et al., 2024; Zhao et al., 2024). Similarly, the influence of seafloor geomorphic features on %OC levels reflects how the seafloor morphology, including features such as mounds, depressions, and canyons, impacts water movement and thereby deposition, erosion, and degradation (e.g., Bao et al., 2018; Sun et al., 2024; Wei et al., 2022). In particular, geomorphic features that reduce hydrodynamic energy and create low-turbulence zones, such as submarine canyons, can enhance OC retention and accumulation (de Haas et al., 2002; LaRowe et al., 2020). Therefore, regions characterized by low wave exposure and specific seafloor geomorphic features tend to exhibit higher sediment OC content, which can be attributed to: (a) increased sedimentation rates allowing a larger fraction of OC to reach the sediment, (b) reduced resuspension and remobilization of the OC already deposited which also minimizes physical reworking and oxygen exposure time slowing down degradation (Blair

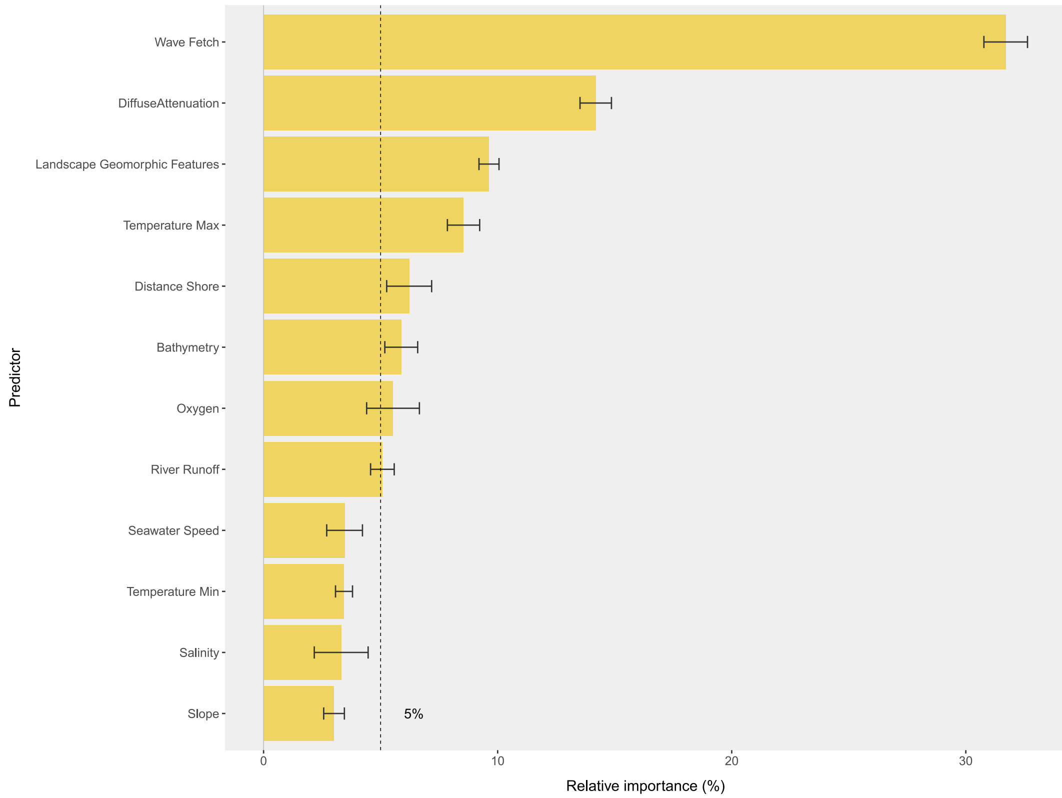

Figure 4. Average (in %; ±standard deviation) relative importance of different relevant environmental predictor variables extracted from the Biological and Oceanographic Rasters for Analysis of Climate and Environmental data set (Bio-ORACLE v3.0) on the sediment percentage organic carbon (%OC) content in European regional seas.

& Aller, 2012), and (c) generally increased water stratification which can promote seasonal hypoxia slowing down the sediment OC degradation (Lee, 1992).

The observed link between higher light diffuse attenuation coefficients and elevated OC in our analysis may be explained by several non-exclusive mechanisms. The diffuse attenuation coefficient quantifies the rate at which light diminishes as it penetrates the water column and is therefore a key determinant of the depth at which photosynthesis can occur (Kirk, 1994). The coefficient is influenced by the amounts of optically active substances (e.g., phytoplankton, colored dissolved organic matter, and inorganic particles; Bowers et al., 2004), and diffuse attenuation typically decreases with distance from shore. Our finding that higher diffuse attenuation (i.e., more turbid waters), typical of coastal waters, was associated with elevated sediment OC suggests that these areas, characterized by higher terrestrial inputs and sedimentation rates, tend to accumulate more OC. Additionally, elevated diffuse attenuation in some offshore regions may reflect localized increased biological activity and enhanced export production (Buesseler et al., 2007), which could also contribute to higher sediment OC levels offshore.

Maximum bottom water temperature also emerged as a key environmental predictor in our analysis, with warmer conditions associated with lower sediment OC content. This relationship was supported by previous studies showing that temperature influences OC storage both directly and indirectly. In deeper waters, elevated temperatures intensify surface water stratification, thereby reducing the upward movement of nutrient-rich water from deeper layers into the surface, leading to potential nutrient limitation of primary production, which can result in a reduced vertical flux of OC to the sediments (Sarmiento et al., 2004). Temperature also affects the rate of metabolism, composition and productivity of planktonic and benthic communities, which in turn influences OC delivery to sediments (Gillooly et al., 2001). Moreover, microbial degradation of OC is temperature-dependent, with higher temperatures increasing the degradation rate of OC (Lønborg et al., 2018). Temperature also affects oxygen dynamics both directly, by modulating oxygen solubility, and indirectly, by altering respiration rates and ocean ventilation (Robinson, 2019). Oxygen availability is an important factor regulating sediment OC

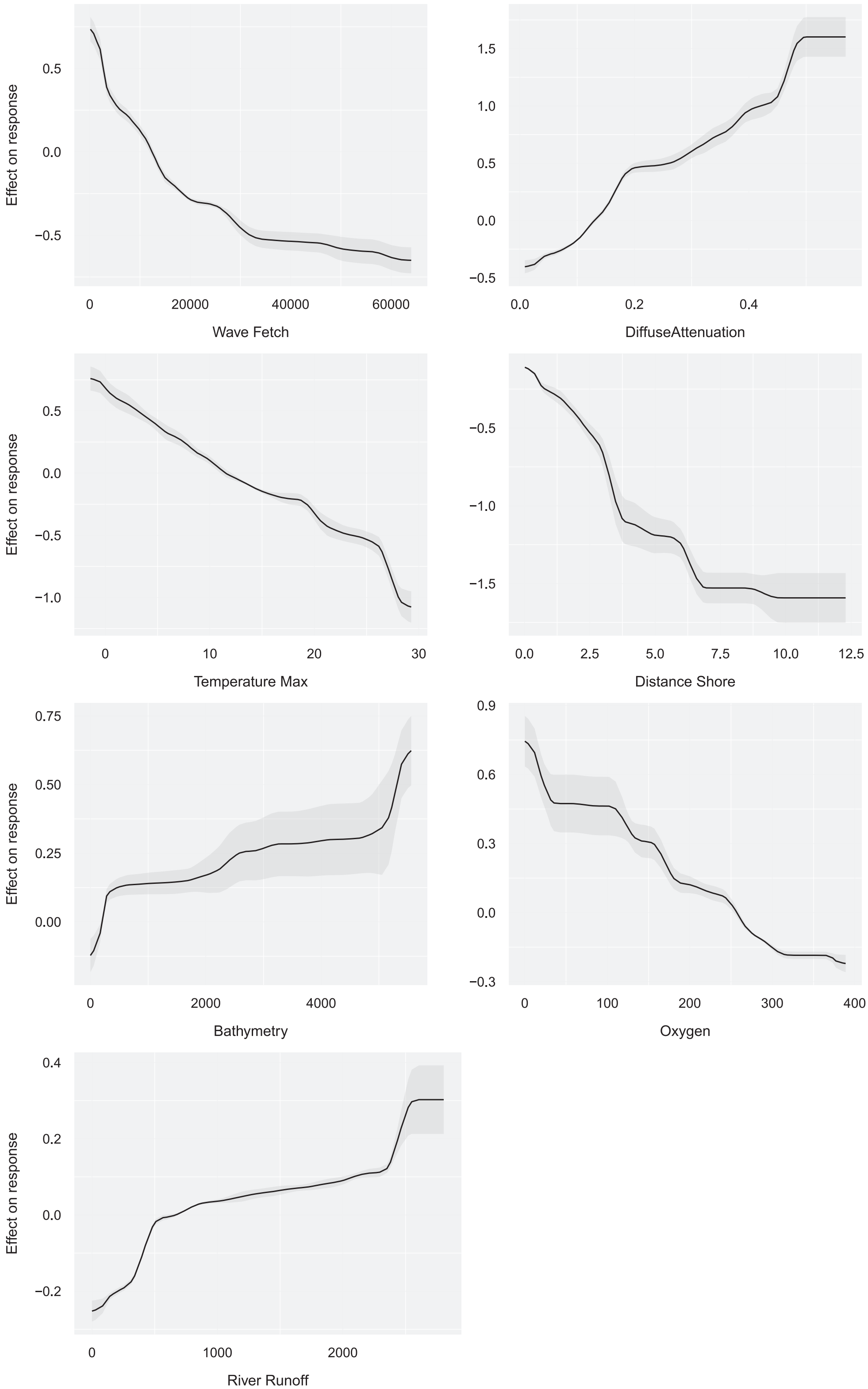

Figure 5. Partial dependency plots depicting the individual effect of each environmental predictor variable extracted from the Biological and Oceanographic Rasters for Analysis of Climate and Environmental data set (Bio-ORACLE v3.0) on the sediment percentage organic carbon (%OC) content in European regional seas.

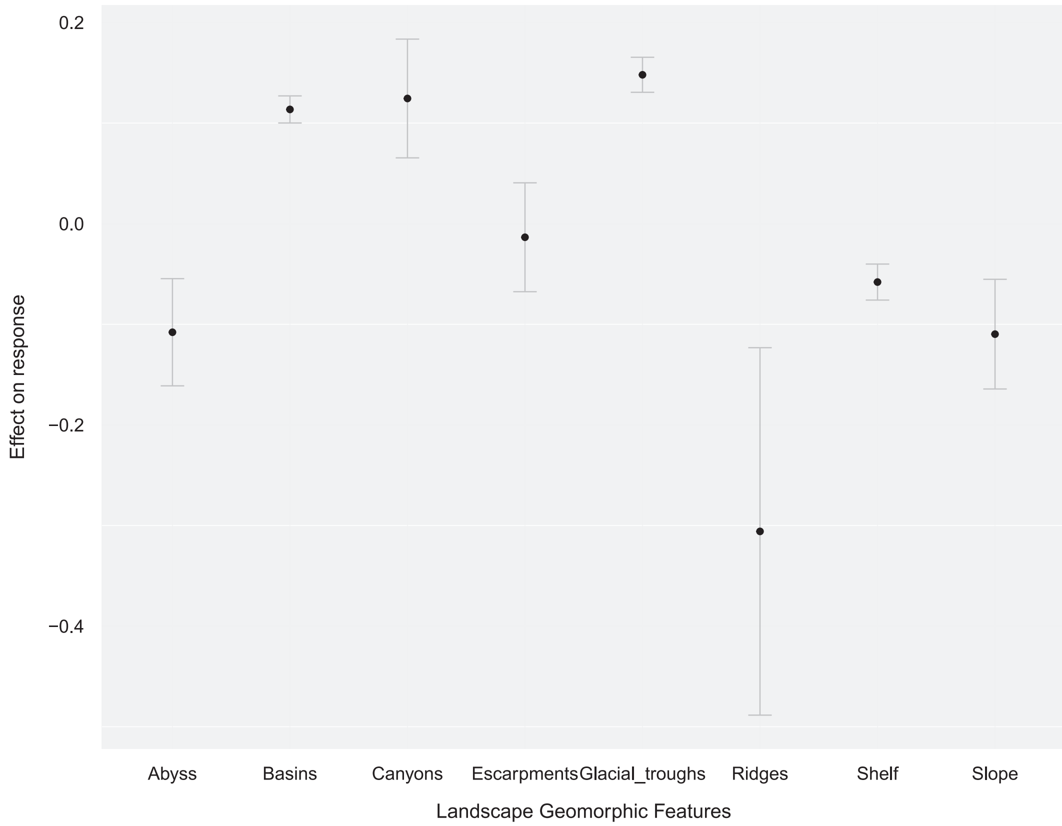

Figure 6. Partial dependency plots depicting the average (shaded areas are ± standard deviation) positive and negative effects of different landscape geomorphic features (abyssal, basins, canyons, escarpments, glacial troughs, ridges, shelves and slopes) predictor variables on the sediment percentage organic carbon (%OC) content in European regional seas.

degradation, with anoxic conditions (0 μmol O_2 L^{-1}) generally leading to slower and less efficient degradation compared to oxic conditions (>60 μmol O_2 L^{-1}) (Jessen et al., 2017). However, some studies suggest that OC degradation rates may be similar under oxic and anoxic conditions (Lee, 1992). Overall, our results indicate that elevated temperatures reduce the sediment OC content. This likely reflects the combined influence of reduced OC delivery, altered biological production, enhanced macrofaunal bioturbation, microbial degradation, and changes in oxygen availability. However, our analysis does not allow us to determine the relative importance of these individual processes on sediment OC.

4.2. Spatial Variability and Relationships

Our map of the spatial distribution of sediment OC content across European regional seas (Figure 8a) clearly showed that %OC levels were higher in inshore regions compared to offshore regions, with elevated levels in the Baltic Sea, North Sea, Adriatic Sea, Barents Sea and Black Sea (Figure 8a). These patterns could largely be explained by nearshore freshwater land runoff and greater inputs of OC from terrestrial sources (Burdige, 2005). Additionally, coastal waters have higher primary productivity, both planktonic and benthic, largely driven by nutrient inputs from rivers and in places upwelling (Lønborg et al., 2021), which increases the flux of OC to coastal sediments. In contrast, in the open (offshore) ocean, only a small fraction of the OC produced in the sunlit surface layers reaches the sediment due to longer degradation pathways and physical dispersion (Buesseler et al., 2007). Furthermore, inshore sediments are more exposed to hydrodynamic forces such as waves, tides, and currents, which affect the transport, resuspension, deposition and degradation of OC (Bao et al., 2018; de Haas et al., 2002; Sun et al., 2024). Therefore, our findings, suggest that wave- and current-sheltered environments (e.g., fjords and bays) have higher sediment OC content, whereas wave-exposed systems (e.g., rocky intertidal habitats) with frequent resuspension, effective sediment sorting toward coarser material, and larger export, have lower OC content (Bao et al., 2018; de Haas et al., 2002). Especially high-energy regions, with repeated cycles of

10.1029/2026GB009100

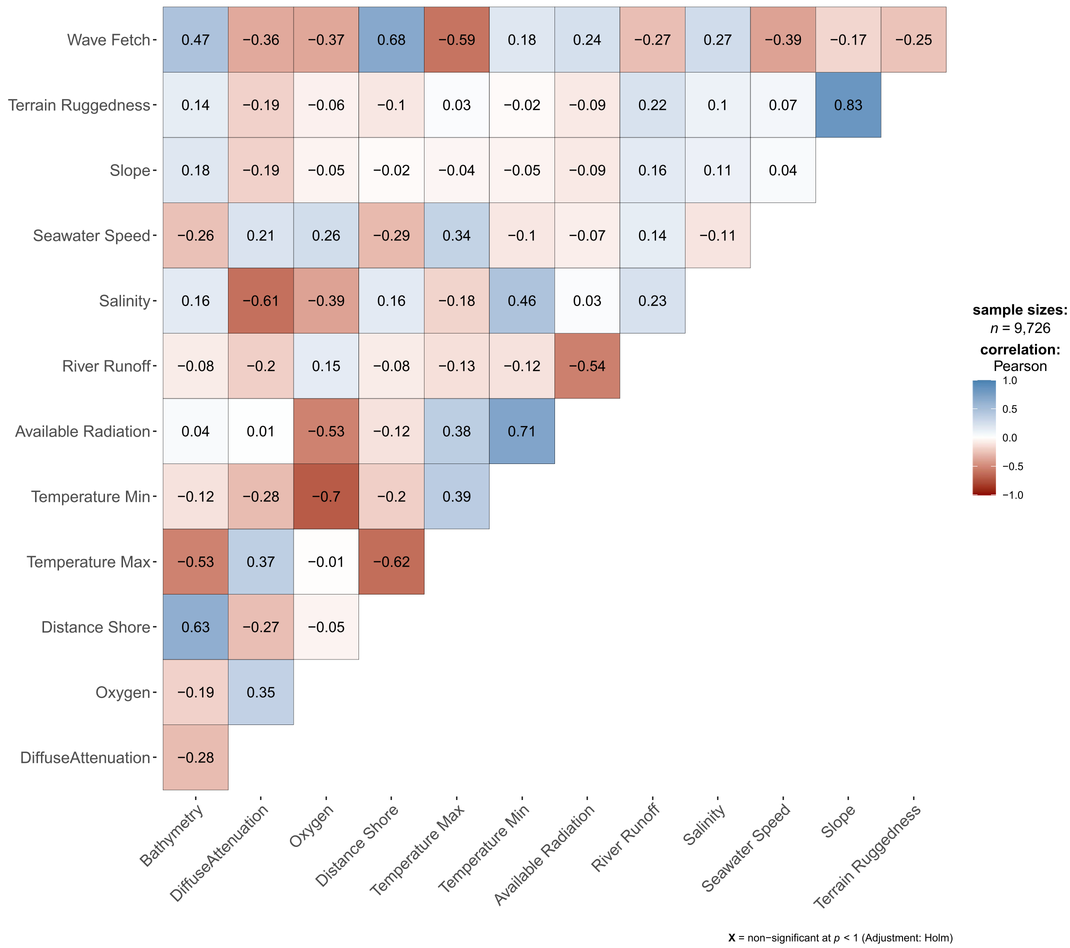

Figure 7. Pearson correlation matrix between all the tested pairs of environmental predictor variables levels in European regional seas which were extracted from Bio-ORACLE v3.0. Color indicates correlation strength and positive/negative direction.

sediment erosion and redeposition, are effective at degrading OC, with studies showing that more than 95% of the OC supplied by primary production and riverine inputs can be degraded within these systems (de Haas et al., 2002). The influence of these processes on the sediment OC was also, as discussed above, reflected in the identified relationship between sediment OC and wave fetch, and to a lesser extent river input, though the latter only explained a minor part of the observed variability.

The relationship between %OC and OC stocks observed in our study (Figure 1) suggests that %OC may serve as a coarse proxy for OC storage in sediments across large data sets, especially when levels are relatively low. However, it does not fully capture OC stocks, as DBD has a strong influence on stock calculations (e.g., Chatting et al., 2025), which is critical for estimating inventories. Because the OC stocks were calculated from the %OC and DBD (or the total dry mass of the sediment), they were inherently related. In addition, our study showed large variability in %OC, and DBD, which varied both spatially and temporally depending on the sediment grain size and packing, which can be influenced by processes such as wave action and bioturbation (Flemming & Delafontaine, 2000).

Matching the locations of individual sediment samples with habitat information from broad-scale maps revealed substantial variability in OC content within each group (Tables 2 and 3; Figure 2). Sediment OC content can vary considerably over small spatial scales due to factors such as local differences in grain size, hydrodynamic regime, terrestrial input, organic matter supply, and benthic faunal activity. In addition, the broad-scale habitat and substrata maps used in this study represent generalized classifications derived from a combination of models, interpolations, and heterogeneous data sources, which limit their representation of local fine-scale variability or

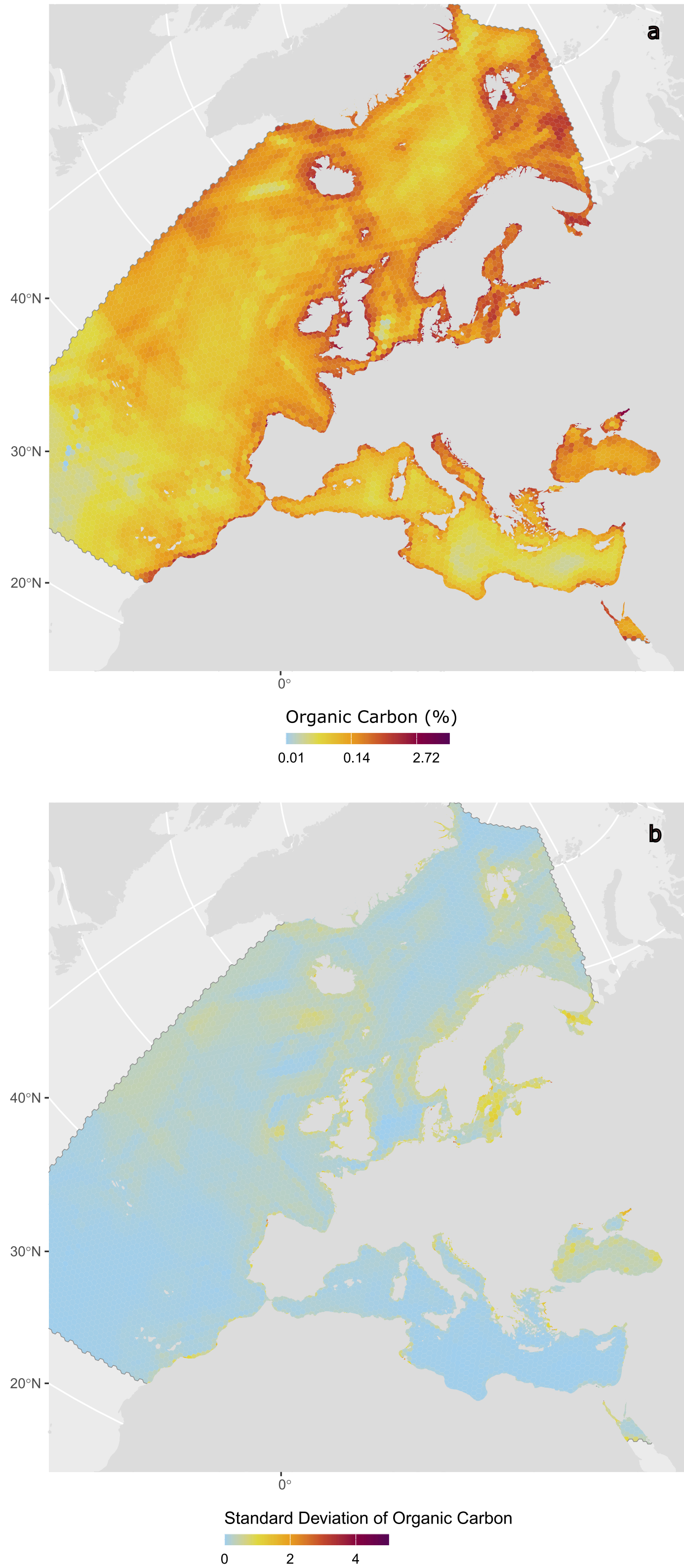

Figure 8. Maps showing the model predicted (a) percentage organic carbon (%OC) and (b) prediction uncertainty, the standard deviation, across the seven bootstrap models. Higher values in (b) indicate less agreement among models and therefore higher associated uncertainty. The maps are presented using a hexagonal grid, where each hexagon has a centroid spacing of 50 km and an edge length of approximately 28.87 km, corresponding to an area of 2165.06 km^2. Spatial patterns in model error are presented in Figure S5 in Supporting Information S1.

patchiness in sediment characteristics. This natural variability, together with the scale mismatch between individual sampling points and broad-scale habitat maps, as well as classification uncertainty, likely contributes to the observed within-class variability and it makes it uncertain when linking sediment OC to mapped seabed habitats. Sediments associated with *P. oceanica* and other seagrass meadows had slightly elevated OC levels relative to other habitats. This observation aligns with previous studies highlighting the role of vegetated marine habitats, particularly *P. oceanica* meadows, as important OC stores (e.g., Mcleod et al., 2011). The reason for different OC storage capacity in vegetated compared to unvegetated areas is because seagrass attenuates wave energy, promotes sedimentation, and thereby regulates sediment properties and facilitates sediment OC storage, while their roots and rhizomes also stabilize the sediments and reduce resuspension (Vizzini et al., 2019). The ability of *P. oceanica* meadows to build up sediments, via vertical growth of the underground structures, makes these meadows more efficient than other seagrass meadows in storing OC (Fourqurean et al., 2012). However, despite the generally higher OC content observed in vegetated habitats, our data show considerable variability within these systems, reflecting local spatial heterogeneity in the conditions. As such, individual sediment samples from vegetated areas may exhibit OC levels comparable to, or even lower than, those from unvegetated habitats, as evident in our study (Tables 2 and 3).

4.3. Uncertainties and Variability

Our analysis is based on direct finer scale measurements of sediment %OC (Graversen et al., 2025) combined with environmental and substrata data, including observations, models and climatology, at much coarser resolution (Assis et al., 2023; Vasquez et al., 2023). This difference in resolution and data type is important to consider when interpreting the variability in OC, as they introduce uncertainty in our results. To address this, we early on in our machine learning analysis tested if using a finer (200 vs. 1,000 m pixels; data not shown) resolution would improve the predictions. While the overall drivers, trends and conclusions were comparable for both resolutions, the model error increased at a finer scale. Because the visual fit of modeled versus measured OC increased with a coarser resolution, this was used in our analysis.

Model predictions of sediment OC showed spatial differences in the uncertainty, with higher uncertainties observed in the North-East Atlantic Ocean, the Black Sea, and inshore regions. The higher uncertainty in the North-East Atlantic Ocean and Black Sea is likely due to the limited availability of sediment OC data, which increases uncertainty in the model predictions. In contrast, higher uncertainty observed in coastal areas is likely linked to factors such as the naturally high environmental variability, differences in OC inputs and dominant habitat, which result in larger sediment OC variability and consequently model uncertainty. Despite this variability, the model did not show any systematic over- or under-prediction in any specific geographic region (Figure 8). This suggests that the model effectively captures broad scale patterns, but is unable to fully account for the very large spatial variability in sediment OC levels.

An important factor known to influence sediment OC levels is the composition of inorganic particles (e.g., clay, silt, carbonates) (Keil & Mayer, 2014). Unfortunately, we were unable to include this in our analysis due to the limited amounts of data (only 8.7% of the OC observations contained information regarding grain size). Clay particles, owing to their high surface area, have a greater capacity to absorb organic matter, often resulting in elevated sediment OC levels, as also shown for our mud sediment class (Table 2). In contrast, sediments dominated by sand typically exhibit lower OC content due to their reduced surface area and weaker adsorption potential, as also evident for our "coarse sand" sediment class (Table 2). Adsorption of OC onto mineral surfaces can protect organic matter from microbial breakdown and thereby enhance OC preservation. Inorganic mineral composition also influences sediment redox gradients and oxygen accessibility, both of which influence OC degradation. These factors were not directly considered in our analysis. However, the distribution, transport, and deposition of inorganic particles are influenced by factors such as wave fetch and sediment class already considered in our analysis. Thus, some of the effects of mineral composition may be indirectly captured through these broader environmental variables. It is also important to recognize that sediment OC content can vary due to local-scale factors not accounted for in our analysis. For example, the presence of bioturbating organisms can increase sediment oxygen uptake and permeability, thereby reducing OC and the accumulation of reduced compounds in sediment pore water (Volkenborn et al., 2007).

Our study provided a reasonable assessment of the main drivers and patterns of sediment OC content across European regional seas. This information is particularly valuable in the context of proposing large networks of

MPAs, where protecting OC-rich sediments can help ensure long-term OC retention as one component of MPA priorities. However, OC content alone is insufficient to inform conservation prioritization and management of OC retention. As areas with higher and lower OC will represent habitats with different species, and conservation aims to protect all species, areas with high OC can only include a subset of the fauna and flora. Indeed, some areas with high OC may be hypoxic or anoxic, and thus have low biodiversity. Factors such as OC reactivity, OC accumulation rates, OC stocks (requiring associated information on DBD), existing anthropogenic pressures, recovery potential, and interactions with biodiversity are also critical when evaluating the effectiveness of measures such as MPAs. Additionally, the spatial resolution and associated uncertainty of the underlying data should be considered, as management decisions are often made at scales that may not align with the data used in this analysis. Our findings also have implications for management relating to the sensitivity of sediment OC to climate change, such as rising sea levels and temperatures, and to damaging human activities such as bottom trawling and dredging, which can impact sediment OC (Epstein et al., 2022; Lønborg et al., 2024). However, it is important to note that our analysis focused on large-scale patterns and found high local-scale heterogeneity. As such, local biological and environmental influences, including variations in species abundance, hydrodynamics, microclimate, and geomorphology, are not fully captured. Therefore, caution is required when applying these findings to smaller site-specific management contexts.

To improve the mapping and prediction of controls on sediment OC, we suggest that future data sets should include additional ancillary data such as DBD and sediment nutrient content (nitrogen and phosphorus). These variables are often lacking but are important for providing a better process understanding and improving model performance. Furthermore, the use of more advanced algorithms (e.g., AI-based approaches) could refine OC predictions.

5. Conclusions

Our results demonstrate that the primary environmental predictors of sediment OC at large spatial scales are wave exposure, light transparency, seafloor geomorphic features, and maximum temperature. The highest OC contents were generally observed in *P. oceanica* and other seagrass meadows as well as in mud, and mixed sediment substrata. The predicted sediment OC across European regional seas indicated elevated levels, particularly in inshore areas and in the Baltic Sea, North Sea, Adriatic Sea, Barents Sea, and the Black Sea. Therefore, OC rich spots tend to occur in inshore regions characterized by low wave exposure and colder temperatures, in vegetated habitats and in submarine canyons.

Conflict of Interest

The authors declare no conflicts of interest relevant to this study.

Availability Statement

The sediment organic carbon data set used in this article is available as a *.csv merged file from the ZENODO database (https://doi.org/10.5281/zenodo.17512391; Lønborg et al., 2025). Environmental data sets used include the Biological and Oceanographic Rasters for Analysis of Climate and Environmental data set (Bio-ORACLE v3.0, https://www.bio-oracle.org/downloads-to-email.php; Assis et al., 2024), Bathymetric predictors (https://bluehabitats.org/?page_id=58; Harris et al., 2014), average annual surface runoff (https://www.earthdata.nasa.gov/data/catalog/ornl-cloud-rivdis-199-1; Fekete et al., 2002), wave exposure (https://figshare.com/articles/Wave_fetch_GIS_layers_for_Europe_at_100m_scale/8668127; Burrows et al., 2023), seabed maps (EMODnet product catalogue; Vasquez et al., 2023) and the EMODnet Geology seabed map (EMODnet product catalogue; Kaskela et al., 2019).

Acknowledgments

The authors thank the associated editor and two anonymous reviewers for their constructive comments and useful suggestions, which have greatly improved the manuscript. This study was funded by the MPA Europe project, which is co-funded by the European Union under the Horizon Europe programme (Grant Agreement: 101059988). UK participants in the Horizon Europe Project MPA Europe were supported by UKRI Grants 10067934 JNCC and 10069750 SAMS. The study also received support from the FCT—Foundation for Science and Technology—through projects UIDP/04326/2020 (https://doi.org/10.54499/UIDP/04326/2020), LA/P/0101/2020 (https://doi.org/10.54499/LA/P/0101/2020), and Scientific Employment Stimulus 2022.00861.CEECIND/CP1729/CT0003 (https://doi.org/10.54499/2022.00861.CEECIND/CP1729/CT0003).

References

Assis, J., Fernández Bejarano, S. J., Salazar, V. W., Schepers, L., Gouvêa, L., Fragkopoulou, E., et al. (2024). Bio-ORACLE v3.0. Pushing marine data layers to the CMIP6 Earth System Models of climate change research [Dataset]. *Global Ecology and Biogeography*, *33*(4), e13813. https://doi.org/10.1111/geb.13813

Assis, J., Neiva, J., Bolton, J. J., Rothman, M. D., Gouveia, L., Paulino, C., et al. (2022). Ocean currents shape the genetic structure of a kelp in southwestern Africa. *Journal of Biogeography*, *49*(5), 822–835. https://doi.org/10.1111/jbi.14338

Assis, J., Sunni, H.-K., Addamo, A. M., & Costello, M. J. (2023). Environmental data preparation. *Nord University, MPA Europe Project Report Deliverable 2.1*, 9.

Atwood, T. B., Witt, A., Mayorga, J., Hammill, E., & Sala, E. (2020). Global patterns in marine sediment carbon stocks. *Frontiers in Marine Science*, *7*, 165. https://doi.org/10.3389/fmars.2020.00165

Bao, R., van der Voort, T. S., Zhao, M., Guo, X., Montluçon, D. B., McIntyre, C., & Eglinton, T. I. (2018). Influence of hydrodynamic processes on the fate of sedimentary organic matter on continental margins. *Global Biogeochemical Cycles*, *32*(9), 1420–1432. https://doi.org/10.1029/2018gb005921

Blair, N. E., & Aller, R. C. (2012). The fate of terrestrial organic carbon in the marine environment. *Annual Review of Marine Science*, *4*(1), 401–423. https://doi.org/10.1146/annurev-marine-120709-142717

Bowers, D. G., Evans, D., Thomas, D. N., Ellis, K., & Williams, P. J. L. B. (2004). Interpreting the colour of an estuary. *Estuarine, Coastal and Shelf Science*, *59*(1), 13–20. https://doi.org/10.1016/j.ecss.2003.06.001

Buesseler, K. O., Lamborg, C. H., Boyd, P. W., Lam, P. J., Trull, T. W., Bidigare, R. R., et al. (2007). Revisiting carbon flux through the ocean's twilight zone. *Science*, *316*(5824), 567–570. https://doi.org/10.1126/science.1137959

Burdige, D. J. (2005). Burial of terrestrial organic matter in marine sediments: A re-assessment. *Global Biogeochemical Cycles*, *19*(4), GB4011. https://doi.org/10.1029/2004gb002368

Burdige, D. J. (2007a). *Geochemistry of marine sediments*. Princeton University Press.

Burdige, D. J. (2007b). Preservation of organic matter in marine sediments: Controls, mechanisms, and an imbalance in sediment organic carbon budgets? *Chemical Review*, *107*(2), 467–485. https://doi.org/10.1021/cr050347q

Burrows, M., Heikes-Knapton, S., Addamo, A. M., & Costello, M. J. (2023). Paper on wave exposure index [Dataset]. *Nord University, MPA Europe Project Report Deliverable 2.2*, 25. https://zenodo.org/records/17590383

Burrows, M. T. (2012). Influences of wave fetch, tidal flow and ocean colour on subtidal rocky communities. *Marine Ecology Progress Series*, *445*, 193–207. https://doi.org/10.3354/meps09422

Burrows, M. T., Harvey, R., & Robb, L. (2008). Wave exposure indices from digital coastlines and the prediction of rocky shore community structure. *Marine Ecology Progress Series*, *353*, 1–12. https://doi.org/10.3354/meps07284

Canfield, D. E. (1994). Factors influencing organic carbon preservation in marine sediments. *Chemical Geology*, *114*(3), 315–329. https://doi.org/10.1016/0009-2541(94)90061-2

Chatting, M., Diesing, M., Hunter, W. R., Grey, A., Kelleher, B. P., & Coughlan, M. (2025). Improving marine sediment carbon stock estimates: The role of dry bulk density and predictor adjustments. *Biogeosciences*, *22*(20), 5975–5990. https://doi.org/10.5194/bg-22-5975-2025

Davies, C. E., Moss, D., & Hill, M. O. (2004). EUNIS habitat classification revised 2004 [Dataset]. *Report to: European environment agency-European topic centre on nature protection and biodiversity*, 127–143. https://www.researchgate.net/publication/238708061_EUNIS_habitat_classification_revised_2004

de Haas, H., van Weering, T. C. E., & de Stigter, H. (2002). Organic carbon in shelf seas: Sinks or sources, processes and products. *Continental Shelf Research*, *22*(5), 691–717. https://doi.org/10.1016/s0278-4343(01)00093-0

Diesing, M., Kröger, S., Parker, R., Jenkins, C., Mason, C., & Weston, K. (2017). Predicting the standing stock of organic carbon in surface sediments of the North–West European continental shelf. *Biogeochemistry*, *135*(1), 183–200. https://doi.org/10.1007/s10533-017-0310-4

Diesing, M., Smeaton, C., Bjarnadóttir, L. R., & Thorsnes, T. (2025). Hotspots and coldspots of seabed organic carbon on the Norwegian continental margin. *Environmental Research Communications*, *7*(10), 105030. https://doi.org/10.1088/2515-7620/ae14bc

Dunne, J. P., Sarmiento, J. L., & Gnanadesikan, A. (2007). A synthesis of global particle export from the surface ocean and cycling through the ocean interior and on the seafloor. *Global Biogeochemical Cycles*, *21*(4), GB4006. https://doi.org/10.1029/2006gb002907

Epstein, G., Middelburg, J. J., Hawkins, J. P., Norris, C. R., & Roberts, C. M. (2022). The impact of mobile demersal fishing on carbon storage in seabed sediments. *Global Change Biology*, *28*(9), 2875–2894. https://doi.org/10.1111/gcb.16105

Eyring, V., Gillett, N., Achutarao, K., Barimalala, R., Barreiro Parrillo, M., Bellouin, N., et al. (2021). Human influence on the climate system. In *Climate Change 2021: The Physical Science Basis. Contribution of Working Group I to the Sixth Assessment Report of the Intergovernmental Panel on Climate Change*, *IPCC sixth assessment report*.

Fekete, B. M., Vörösmarty, C. J., & Grabs, W. (2002). High-resolution fields of global runoff combining observed river discharge and simulated water balances [Dataset]. *Global Biogeochemical Cycles*, *16*(3), 15-1–15-10. https://doi.org/10.1029/1999gb001254

Flemming, B. W., & Delafontaine, M. T. (2000). Mass physical properties of muddy intertidal sediments: Some applications, misapplications and non-applications. *Continental Shelf Research*, *20*(10), 1179–1197. https://doi.org/10.1016/s0278-4343(00)00018-2

Fourqurean, J. W., Duarte, C. M., Kennedy, H., Marbà, N., Holmer, M., Mateo, M. A., et al. (2012). Seagrass ecosystems as a globally significant carbon stock. *Nature Geoscience*, *5*(7), 505–509. https://doi.org/10.1038/ngeo1477

Gattuso, J.-P., Heymans, S., Natalie, H., Neukermans, G., Landschützer, P., & Pörtner, H.-O. (2023). *Blue Carbon: Challenges and opportunities to mitigate the climate and biodiversity crises* Report. European Marine Board.

Gillooly, J. F., Brown, J. H., West, G. B., Savage, V. M., & Charnov, E. L. (2001). Effects of size and temperature on metabolic rate. *Science*, *293*(5538), 2248–2251. https://doi.org/10.1126/science.1061967

Gouvêa, L., Fragkopoulou, E., Legrand, T., Serrão, E. A., & Assis, J. (2024). Range map data of marine ecosystem structuring species under global climate change. *Data in Brief*, *52*, 110023. https://doi.org/10.1016/j.dib.2023.110023

Graversen, A. E. L., Lønborg, C., Addamo, A. M., Pedersen, S. G., Chemello, S., Alejo, I., et al. (2025). A marine and salt marsh sediment organic carbon database for European regional seas (EURO-CARBON). *Data in Brief*, *60*, 111595. https://doi.org/10.1016/j.dib.2025.111595

Harris, P. T., Macmillan-Lawler, M., Rupp, J., & Baker, E. K. (2014). Geomorphology of the oceans [Dataset]. *Marine Geology*, *352*, 4–24. https://doi.org/10.1016/j.margeo.2014.01.011

Howard, J., Sutton-Grier, A. E., Smart, L. S., Lopes, C. C., Hamilton, J., Kleypas, J., et al. (2023). Blue carbon pathways for climate mitigation: Known, emerging and unlikely. *Marine Policy*, *156*, 105788. https://doi.org/10.1016/j.marpol.2023.105788

Jessen, G. L., Lichtschlag, A., Ramette, A., Pantoja, S., Rossel, P. E., Schubert, C. J., et al. (2017). Hypoxia causes preservation of labile organic matter and changes seafloor microbial community composition (Black Sea). *Science Advances*, *3*(2), e1601897. https://doi.org/10.1126/sciadv.1601897

Kaskela, A. M., Kotilainen, A., Alanen, U., Cooper, R., Green, S., Guinan, J., et al. (2019). Picking up the pieces—Harmonising and collating seabed substrate data for European maritime areas [Dataset]. *Geosciences*, *9*(2), 84. https://doi.org/10.3390/geosciences9020084

Keil, R. G., & Mayer, L. M. (2014). Mineral matrices and organic matter. In H. Holland & K. Turekian (Eds.), *Treatise on geochemistry* (2nd ed., pp. 337–359). Elsevier.

Kirk, J. T. O. (1994). *Light and photosynthesis in aquatic ecosystems* (2nd ed.). Cambridge University Press.

Lamichhane, S., Kumar, L., & Wilson, B. (2019). Digital soil mapping algorithms and covariates for soil organic carbon mapping and their implications: A review. *Geoderma*, *352*, 395–413. https://doi.org/10.1016/j.geoderma.2019.05.031

LaRowe, D. E., Arndt, S., Bradley, J., Estes, E., Hoarfrost, A., Lang, S., et al. (2020). The fate of organic carbon in marine sediments—New insights from recent data and analysis. *Earth-Science Reviews*, *204*, 103146. https://doi.org/10.1016/j.earscirev.2020.103146

Lee, C. (1992). Controls on organic carbon preservation: The use of stratified water bodies to compare intrinsic rates of decomposition in oxic and anoxic systems. *Geochimica et Cosmochimica Acta*, *56*(8), 3323–3335. https://doi.org/10.1016/0016-7037(92)90308-6

Lønborg, C., Álvarez–Salgado, X. A., Letscher, R. T., & Hansell, D. A. (2018). Large stimulation of recalcitrant dissolved organic carbon degradation by increasing ocean temperatures. *Frontiers in Marine Science*, *4*, 436. https://doi.org/10.3389/fmars.2017.00436

Lønborg, C., Graversen, A. E. L., Addamo, A. M., Pedersen, S. G., Chemello, S., Alejo, I., et al. (2025). EURO-Carbon full data set [Dataset]. *Zenodo*. https://doi.org/10.5281/zenodo.17512391

Lønborg, C., Markager, S., Herzog, S. D., Carreira, C., & Høgslund, S. (2024). Impacts of anthropogenic resuspension on sediment organic matter: An experimental approach. *Estuarine, Coastal and Shelf Science*, *310*, 108981. https://doi.org/10.1016/j.ecss.2024.108981

Lønborg, C., Müller, M., Butler, E. C., Jiang, S., Ooi, S. K., Trinh, D. H., et al. (2021). Nutrient cycling in tropical and temperate coastal waters: Is latitude making a difference? *Estuarine, Coastal and Shelf Science*, *262*, 107571. https://doi.org/10.1016/j.ecss.2021.107571

Mcleod, E., Chmura, G. L., Bouillon, S., Salm, R., Björk, M., Duarte, C. M., et al. (2011). A blueprint for blue carbon: Toward an improved understanding of the role of vegetated coastal habitats in sequestering CO_2. *Frontiers in Ecology and the Environment*, *9*(10), 552–560. https://doi.org/10.1890/110004

R Core Team. (2023). R: A language and environment for statistical computing [Software]. *R Foundation for Statistical Computing*. Retrieved from https://www.r-project.org/

Robinson, C. (2019). Microbial respiration, the engine of ocean deoxygenation. *Frontiers in Marine Science*, *5*, 533. https://doi.org/10.3389/fmars.2018.00533

Sarmiento, J. L., Slater, R., Barber, R., Bopp, L., Doney, S. C., Hirst, A. C., et al. (2004). Response of ocean ecosystems to climate warming. *Global Biogeochemical Cycles*, *18*(3), GB3003. https://doi.org/10.1029/2003gb002134

Smeaton, C., & Austin, W. E. N. (2022). Quality not quantity: Prioritizing the management of sedimentary organic matter across continental shelf seas. *Geophysical Research Letters*, *49*(5), e2021GL097481. https://doi.org/10.1029/2021gl097481

Sun, X., Hu, L., Fan, D., Wang, H., Yang, Z., & Guo, Z. (2024). Sediment resuspension accelerates the recycling of terrestrial organic carbon at a large river-coastal ocean interface. *Global Biogeochemical Cycles*, *38*(7), e2024GB008213. https://doi.org/10.1029/2024gb008213

Tegler, L. A., Horner, T. J., Galy, V., Bent, S. M., Wang, Y., Kim, H. H., et al. (2024). Distribution and drivers of organic carbon sedimentation along the continental margins. *AGU Advances*, *5*(4), e2023AV001000. https://doi.org/10.1029/2023av001000

Vasquez, M., Ségeat, B., Cordingley, A., Tilby, E., Wikström, S., Ehrnsten, E., et al. (2023). EUSeaMap 2023, A European broad-scale seabed habitat map, Technical Report [Dataset]. *ARCHIMER*. https://archimer.ifremer.fr/doc/00859/97116/

Vizzini, S., Apostolaki, E. T., Ricevuto, E., Polymenakou, P., & Mazzola, A. (2019). Plant and sediment properties in seagrass meadows from two Mediterranean CO_2 vents: Implications for carbon storage capacity of acidified oceans. *Marine Environmental Research*, *146*, 101–108. https://doi.org/10.1016/j.marenvres.2019.03.001

Volkenborn, N., Polerecky, L., Hedtkamp, S., van Beusekom, J. E., & De Beer, D. (2007). Bioturbation and bioirrigation extend the open exchange regions in permeable sediments. *Limnology and Oceanography*, *52*(5), 1898–1909. https://doi.org/10.4319/lo.2007.52.5.1898

Wakeham, S. G., & Canuel, E. A. (2006). Degradation and preservation of organic matter in marine sediments. In J. K. Volkman (Ed.), *Marine organic matter: Biomarkers, isotopes and DNA* (pp. 295–321). Springer.

Wei, L., Cai, P., Shi, X., Cai, W.-J., Liu, W., Hong, Q., et al. (2022). Winter mixing accelerates decomposition of sedimentary organic carbon in seasonally hypoxic coastal seas. *Geochimica et Cosmochimica Acta*, *317*, 457–471. https://doi.org/10.1016/j.gca.2021.11.003

Wellsbury, P., Goodman, K., Barth, T., Cragg, B. A., Barnes, S. P., & Parkes, R. J. (1997). Deep marine biosphere fuelled by increasing organic matter availability during burial and heating. *Nature*, *388*(6642), 573–576. https://doi.org/10.1038/41544

Weyer, N. M., Cifuentes-Jara, M., Frölicher, T., Jackson, M., Kudela, R., & Masson-Delmotte, V. (2019). Annex I: Glossary. In *IPCC Special Report on Ocean and Cryosphere in a Changing Climate* (pp. 677–702).

Williamson, P., & Gattuso, J.-P. (2022). Carbon removal using coastal blue carbon ecosystems is uncertain and unreliable, with questionable climatic cost-effectiveness. *Frontiers in Climate*, *4*, 853666. https://doi.org/10.3389/fclim.2022.853666

Wu, G., Nierop, K. G. J., Yang, B., Schouten, S., Reichart, G. J., & Kraal, P. (2026). Perturbation increases source-dependent organic matter degradation rates in estuarine sediments. *Biogeosciences*, *23*(3), 995–1012. https://doi.org/10.5194/bg-23-995-2026

Zhao, B., Yao, P., Wei, Q., Bianchi, T. S., Watts, E. G., Wang, B., & Yu, Z. (2024). Effects of seasonal deposition-erosion cycle on sedimentary organic carbon remineralization and oxygen consumption in a large-river delta-front estuary. *Science of the Total Environment*, *916*, 170377. https://doi.org/10.1016/j.scitotenv.2024.170377